



Published in final edited form as:

Arch Biochem Biophys. 2017 December 01; 635: 17–26. doi:10.1016/j.abb.2017.10.011.

Sex-dependent impact of *Scp-2/Scp-x* gene ablation on hepatic phytol metabolism

Avery L. McIntosh¹, Stephen M. Storey¹, Huan Huang¹, Ann B. Kier², and Friedhelm Schroeder^{1,*}

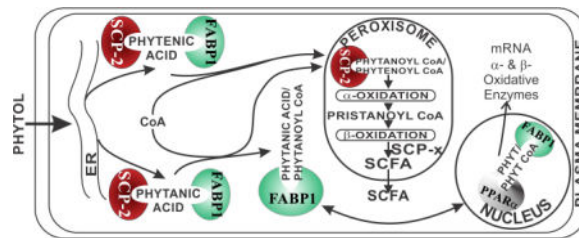
¹Department of Physiology and Pharmacology, Texas A&M University TVMC, College Station, TX 77843-4466

²Department of Pathobiology, Texas A&M University TVMC, College Station, TX 77843-4467

Abstract

While prior studies focusing on male mice suggest a role for sterol carrier protein-2/sterol carrier protein-x (SCP-2/SCP-x; DKO) on hepatic phytol metabolism, its role in females is unresolved. This issue was addressed using female and male wild-type (WT) and DKO mice fed a phytoestrogen-free diet without or with 0.5% phytol. GC/MS showed that hepatic: i) phytol was absent and its branched-chain fatty acid (BCFA) metabolites were barely detectable in WT control-fed mice; ii) accumulation of phytol as well as its peroxisomal metabolite BCFA (phytanic acid >> pristanic and 2,3-pristenic acids) was increased by dietary phytol in WT females, but only slightly in WT males; iii) accumulation of phytol and BCFA was further increased by DKO in phytol-fed females, but much more markedly in males. Livers of phytolfed WT female mice as well as phytol-fed DKO female and male mice also accumulated increased proportion of saturated straight-chain fatty acids (LCFA) at the expense of unsaturated LCFA. Liver phytol accumulation was not due to increased SCP-2 binding/transport of phytol since SCP-2 bound phytanic acid, but not its precursor phytol. Thus, the loss of *Scp-2/Scp-x* contributed to a sex-dependent hepatic accumulation of dietary phytol and BCFA.

Graphical Abstract



*Address correspondence to: Friedhelm Schroeder, Department of Physiology and Pharmacology, Texas A&M University, TVMC, College Station, TX 77843-4466. Telephone: (979) 862-1433, FAX: (979) 862-4929, fschroeder@cvm.tamu.edu.

Publisher's Disclaimer: This is a PDF file of an unedited manuscript that has been accepted for publication. As a service to our customers we are providing this early version of the manuscript. The manuscript will undergo copyediting, typesetting, and review of the resulting proof before it is published in its final citable form. Please note that during the production process errors may be discovered which could affect the content, and all legal disclaimers that apply to the journal pertain.

Keywords

phytol; SCP-2; SCP-x; branched-chain fatty acids; mice; liver

1. Introduction

Humans on average ingest 50–100 mg/day of dietary branched-chain phytol and phytanic acid derived therefrom, almost all of which is rapidly degraded and generally not detectable in serum or tissues of normal individuals [1]. Since the discovery of phytanic acid most attention has focused on resolving the individual enzymatic steps, enzymes, and intracellular organelle localization of phytanic acid metabolism [1–3]. Surprisingly, much less is known about the role of cytosolic proteins responsible for binding/transporting the aqueous very insoluble phytanic acid to its metabolic (peroxisome) and regulatory (nucleus) organelle targets. A key potential candidate gene serving in this regard is the sterol carrier protein-2/sterol carrier protein-x (*Scp-2/Scp-x*) gene which encodes two proteins (SCP-2 and SCP-x) both of which may be involved in BCFA oxidation. These two proteins are related as the protein SCP-x contains the SCP-2 protein in its C-terminus and while SCP-x has enzymatic activity, SCP-2 does not [4]. Despite SCP-2 having no enzymatic activity, it binds phytanic acid [5, 6] and even more tightly phytanoyl-CoA [6]. More importantly, the phytanoyl-CoA/SCP-2 complex serves as the substrate for phytanoyl-CoA-2-hydroxylase in the peroxisomal matrix [7, 8]. Although nearly half of total SCP-2 is localized in the cytoplasm, it is more highly concentrated in peroxisomes [9–11] wherein SCP-2 is associated with fatty acid oxidative enzymes [12]. These findings suggested that SCP-2 may be involved in the cytosolic transfer of phytanic acid from endoplasmic reticulum (site of phytol conversion to phytanic acid) to peroxisomes and potentially to further downstream oxidation therein [5, 6]. Finally, SCP-x is localized exclusively in peroxisomes wherein it is the only known enzyme with branched-chain acyl-CoA 3-ketothiolase activity needed for oxidizing BCFA [13, 14].

Although the *in vivo* significance of *Scp-/Scp-x* gene ablation (DKO) in phytol metabolism has been examined in male mice, nothing is known regarding the impact of DKO in females, especially with regards to phytol vs BCFA metabolite accumulation. Since *Scp-2/Scp-x* gene expression is markedly sexual dimorphic in mice [4, 15], there is a need for such studies in female DKO mice. Although an earlier study reported the impact of DKO on hepatic appearance of BCFA in phytol-fed male mice [6], neither the potential accumulation of phytol nor female mice were examined. However, interpretation of the latter study was complicated by the control diet itself having a high content of phytol and phytanic acid, which lead to potent ligand induction of nuclear receptor transcriptional activity mediated by the heterodimer pair retinoid X receptor (RXR) [16, 17] and peroxisome proliferator activated receptor- α (PPAR α) [18–21]. Hyperactivation of PPAR α results in excessive oxidative stress and cardiac toxicity as seen in a study involving mice overexpressing PPAR α in muscle [22].

To begin to address this issue and examine the impact of sex on phytol metabolism in DKO mice, the current study focused on the impact of DKO on hepatic phytol metabolism in female versus male mice fed a phytol-free, phytanic acid-free control diet without or with

0.5% added phytol. Gas chromatography/mass spectrometry (GC/MS) was used to examine the impact of DKO on phytol diet-induced hepatic accumulation of phytol and peroxisomal BCFA (phytanic acid >> pristanic and 2,3-pristenic acids) metabolites.

2. Materials and Methods

2.1. Materials

Phytol, phytanic acid, pristanic acid, phytanic methyl ester, and *N-tert*-butyldimethylsilyl-*N*-methyltrifluoroacetamide (MBDSTFA) with 1% *tert*-butyldimethylchlorosilane (TBDMSCL) were purchased from Sigma-Aldrich Co. LLC (St. Louis, MO). Purified long chain fatty acid (LCFA) standards were obtained from Nu-Chek Prep, Inc. (Elysian, MN). Pristanic methyl ester (methyl pristanate) was from Larodan AB (Malmo, Sweden). Reagents and solvents used were of the highest grade available and cell culture tested.

2.2. Fluorescence displacement assay to determine SCP-2 affinity for phytol, phytanic acid, and pristanic acid

Recombinant SCP-2 protein was isolated and kept at -80°C as previously described [23]. Phytol and phytanic acid binding to SCP-2 was determined by 12-(*N*-methyl)-*N*-((7-nitrobenz-2-oxa-1,3-diazol-4-yl)amino)-octadecanoic acid (NBD-stearic acid) fluorescence displacement assay as described previously [24, 25]. While NBD-stearic acid very weakly fluoresces in buffer, its fluorescence increases upon binding to proteins such as SCP-2. Thus emission spectra were recorded for both background fluorescence of NBD-stearic acid in buffer and the increase in fluorescence of NBD-stearic acid upon ligand binding to SCP-2. The binding experiments were performed in a quartz cuvette using 10 mM phosphate buffer at $\text{pH}=7.4$ at 24°C . The spectra were recorded by exciting NBD-stearic acid at 490 nm and scanning its emission over the wavelengths from 515–600nm using a Varian Cary Eclipse Fluorescence Spectrophotometer (Varian, Inc, Palo Alto, CA). Forward and reverse titrations were used to determine a K_d of $0.22 \pm 0.03 \mu\text{M}$ for NBD-stearic acid binding to a single binding site per molecule of SCP-2 as described previously [24, 25]. Displacing ligands (e.g. phytol, phytanic acid, pristanic acid) from 2mg/ml stock solution in DMF were titrated into a solution of SCP-2 (500nM) and NBD-stearic acid (500nM) in 10mM phosphate buffer, $\text{pH}=7.4$. Upon binding to SCP-2, the ligands would displace the bound NBD-stearic acid, resulting in decrease of fluorescence. K_i was calculated using the EC_{50} obtained from the displacement curves and the K_d for NBD-stearic acid according to the following equation:

$$K_i = K_d \times EC_{50} / [NBDS].$$

2.3. Animal studies

Male and female *Scp-2/Scp-x* null (double knockout; DKO) mice on the C57BL/6Ncr background (N6 backcross generation) were generated as in [26]. Male and female inbred C57BL/6Ncr wild-type (WT) mice were from the Frederick Cancer Research and Development Center (Frederick, MD). Mice were kept on a consistent diurnal cycle (12h light/12h dark) with free access to water and food. Mice were monitored quarterly for infectious diseases and were specific pathogen free, particularly in reference to mouse hepatitis virus. Animal protocols were approved by the Animal Care and Use Committee of Texas A&M University.

2.4. Phytol dietary study

For the dietary study 28 male and 28 female (7 wk old, 20–30g) WT and DKO mice were placed on diet D11243 (Research Diets, Inc., New Brunswick, NJ), which is an AIN-76A rodent diet modified by Research Diets, Inc. (New Brunswick, NJ) to contain 50% carbohydrates (50% sucrose with remaining as corn starch and maltodextrin) and 5% calories from fat (mainly from corn oil). This control diet was essentially free of phytol, phytanic acid, and phytoestrogens, thereby avoiding potential diet-induced problems with high levels of phytol and phytanic acid in the control diet [6] as well as with phytoestrogens in sex comparisons [27, 28]. After acclimating for 1 week on the modified control diet, the mice were divided into four groups each of which consisted of seven females and seven males: two groups of WT and DKO mice remained on the control diet while the other two groups were switched to the above D11243 rodent diet supplemented with 0.5% phytol (custom diet D01020601; Research Diets, Inc.). Body weight and food intake were monitored every other day. At the end of the study (day 13), animals were fasted overnight, anesthetized (100mg/kg ketamine, 10mg/kg xylazine), and humanely euthanized via cervical dislocation. Harvested serum and liver samples were snap-frozen on dry ice and stored at -80°C .

2.5. Lipid extraction from liver and diet

Small samples of liver and diet were minced thoroughly and homogenized in 0.5ml PBS with a motor-driven pestle (Tekmar Co, Cincinnati, OH) at 2,000rpm, then extracted twice with *n*-hexane:2-propanol (3:2, v/v) [29, 30]. All glassware used for lipid extraction, fatty acid analysis, and phytol analysis was washed with sulfuric acid-chromate before use and lipids were stored under an atmosphere of N_2 to limit oxidation. The lipid extracts from each sample were dried under N_2 followed by base-catalyzed transesterification (1M KOH in methanol at 37°C for 20min) to convert the lipid acyl chains to fatty acid methyl esters (FAMES). Transesterification was stopped with 200 μl ethyl formate and the FAMES were then extracted into petroleum ether and dried under N_2 . For FAME analysis, the esterified fatty acids were dissolved in *n*-hexane with a known amount of pentadecanoic methyl ester (15:0-ME) internal standard. Post-extraction residues dried overnight and digested overnight in 0.2 M KOH were used for protein determination by Bradford assay [31].

2.6. Fatty acid derivatization: transesterification to fatty acid methyl esters (FAME)

An aliquot of the above lipid extracts from each sample were dried under N_2 followed by base-catalyzed transesterification (1M KOH in methanol at 37°C for 20min) to convert the lipid acyl chains to fatty acid methyl esters (FAMES). Transesterification was stopped with 200 μl ethyl formate and the FAMES were then extracted into petroleum ether and dried under N_2 . For FAME analysis, the esterified fatty acids were dissolved in *n*-hexane with a known amount of pentadecanoic methyl ester (15:0-ME) internal standard.

2.7. Gas chromatography/Mass spectrometry (GC/MS) of fatty acid methyl esters (FAME)

FAMES produced above were separated using a Thermo FinniganTrace GC 2000 system (Thermo Fisher Scientific Inc., Waltham, MA) equipped with a RTX-2330 capillary column (0.25 mm inner diameter \times 30 m length; Restek, Bellefonte, PA). FAMES were identified by

comparison of retention times to known standards and confirmed by Trace DSQ version 1.3.1 single quadrupole mass spectrophotometer in chemical ionization and electron ionization modes (Thermo Fisher Scientific Inc., Waltham, MA). FAMES were quantitated using Xcalibur version 1.3 software (Thermo Fisher Scientific, Inc.). Individual peaks were identified by comparison with known FAME, phytanic methyl ester, and pristanic methyl ester standards as well as parental ion molecular weights (chemical ionization mode) and fragmentation pattern (electron ionization mode) matching using the Xcalibur 1.3 ion fragmentation library. Identified FAME peaks were then referenced against the internal standard (15:0-ME) for quantification. FAME mass content was calculated as (nmol/mg protein) or as (% of total fatty acid) as described [32]. The FAME double bond index (DBI) and peroxidizability index were calculated as described [32].

2.8. Phytol derivatization using trimethylsilylation and gas chromatography/mass spectrometry (GC/MS) of trimethylsilylated phytol

For phytol quantification, an aliquot of the above lipid extract from each sample was dissolved in 100 μ l MBDSTFA with 1% TBDMSCL, incubated at 60°C for 2hr, dried under N₂, and dissolved in *n*-hexane similarly as described [33].

Silylated phytol was quantified with the above GC/MS system except using a Rxi-5ms capillary column (0.20mm inner diameter \times 25m length; recommended by Restek) with chemical ionization mass spectrometry and comparison to 15:0-ME internal standard and silylated phytol external standard control curves (chromatograph peak area vs. concentration). A standard curve derived from a set of known amounts of phytol standard (MTBSTFA derivatized, extracted, and quantified by GC-MS) was used to calculate the nmol phytol in the hepatic and diet samples. Phytol mass content was expressed as nmol/mg protein.

2.9 Statistical analysis

Phytol and fatty acid subgrouping values were calculated as the sums of indicated fatty acid/alcohol types (total fatty acids, total branched chain, monounsaturated, etc.) in nmol lipid/mg total liver protein or/mg diet as well as a percent of total liver or diet fatty acids. All values are expressed as means \pm SEM with 'n' indicated. Statistical analysis was performed using one-way ANOVA analysis with Newman-Keuls paired comparisons posttest (GraphPad Prism, San Diego, CA). Values with P \leq 0.05 were considered statistically significant.

3. Results

3.1. Dietary content of phytol

Since standard rodent chow contains significant amount of dietary phytol, e.g. as much as 75 μ g/gram that could complicate interpretation [6], the current study was performed using a commercial defined control-diet (D11243) prepared to be free of phytol and phytanic acid. To assure that this diet was indeed deficient in phytol; lipids were extracted, derivatized, and analyzed by GC/MS as described in Methods. GC/MS of the silylated alcohols in the lipid extract detected only a trace amount of phytol in the control diet representing 0.00028

$\pm 0.000043\%$ by weight or $2.8 \pm 0.004 \mu\text{g/g}$. Further, GC/MS of the 0.5% phytol-supplemented diet (D01020601) confirmed its total phytol content, *i.e.* $0.45 \pm 0.037\%$ by weight or $4.5 \pm 0.4 \text{ mg/g}$.

Taken together, this showed that the control-diet used herein was very low in phytol, 27-fold lower than standard rodent chow [6]. This small amount of phytol did not significantly contribute to raising total phytol content of the 0.5% phytol experimental diet.

3.2. Dietary content of phytol metabolites

Standard control rodent chow also contains even higher levels of phytanic acid, e.g. as much as $200 \mu\text{g/gram}$ [6]. Thus, the phytanic acid content of the control-diet used herein was determined by extracting the lipids, preparing fatty acid methyl esters (FAMES), and resolving and quantitating by GC/MS as described in Methods.

GC/MS of the FAMES revealed that the control diet was deficient in branched-chain fatty acids (BCFA) such as phytanic or pristanic acids. However, the control diet did contain significant amounts of straight-chain fatty acids, primarily C16:0, C18:1, and C18:2, plus small amounts of other fatty acids (Supplemental Table 1). This was consistent with the fatty acid composition provided by request from Research Diets, Inc (New Brunswick, NJ).

In summary, as compared to standard control rodent chow [6], the control diet had no detectable phytol-derived BCFA (*i.e.* phytanic acid, pristanic acid).

3.3. SCP-2 affinity for phytol vs phytanic acid and pristanic acid: NBD-stearic acid fluorescence displacement

Since SCP-2 binds cholesterol, a polycyclic alcohol with a branched-side chain [10, 34, 35], the possibility that SCP-2 may bind dietary phytol to similarly function in uptake/intracellular transport of phytol was considered. However, phytol did not significantly displace SCP-2-bound NBD-stearic acid even at very high levels, *i.e.* $\sim 5 \mu\text{M}$ phytol (Fig 1). The inability of SCP-2 to bind phytol was confirmed with a direct binding assay by measuring tyrosine quenching and by displacement of NBD-cholesterol (not shown). In contrast, SCP-2 had high affinity for phytanic acid ($K_d = 0.49 \pm 0.01 \mu\text{M}$) and pristanic acid ($K_d = 0.50 \pm 0.04 \mu\text{M}$), phytol metabolites produced in the endoplasmic reticulum and peroxisome, respectively (Fig 1). The finding that SCP-2 does not appear to bind phytol, suggests that any impact of SCP-2 on phytol metabolism is likely mediated through SCP-2's effects on downstream metabolism of phytol.

3.4. Impact of Scp-2/Scp-x gene ablation (DKO) on sex-dependence of hepatic phytol content

Although SCP-2 does not bind phytol, it binds phytol metabolites such as phytanic acid (Fig. 1) and its metabolically-activated phytanoyl-CoA thioesters [6]. Further, the phytanoyl-CoA/SCP-2 complex serves as the substrate for phytanoyl-CoA-2-hydroxylase in the peroxisomal matrix [7, 8]. These findings suggested that SCP-2 may influence phytol uptake/accumulation by its impact on downstream phytol oxidation (e.g. to phytanic acid in endoplasmic reticulum and/or within peroxisomes for oxidation). This hypothesis was tested

by measuring various parameters to determine the impact of DKO on sex-dependent hepatic phytol levels in mice fed control vs phytol supplemented diet.

At the end of the study only very low levels of phytol were found in livers of control-fed female and male wild-type (WT) mice, 3.3 ± 0.6 and 2.7 ± 0.6 nmol/mg, respectively (Fig. 2A,B) with no significant difference resulting from the DKO (Fig. 2A,B). Dietary phytol supplementation increased hepatic phytol content by nearly 5-fold to 15 ± 4 nmol/mg in WT females (Fig. 2A) and nearly 7-fold to 20 ± 6 nmol/mg (Fig. 2B) in livers of WT males. DKO did not significantly increase phytol accumulation in phytol-fed females (Fig. 2A) but induced phytol accumulation by 3.6-fold in phytol-fed males (Fig. 2B) when compared to their phytol-fed WT counterparts.

While livers of phytol-fed WT females showed high levels of total branched chain lipids (phytol + BCFA) accumulation, phytol-fed WT males were at least 7.5-fold lower (Fig. 2C,D). DKO increased the hepatic content of total branched-chain lipid in phytol-fed female mice by a mere 1.2-fold (Fig. 2C) and by more than 7-fold in the male mice (Fig. 2D).

Thus, mice exhibit strong sex differences in regards to hepatic accumulation of phytol and total branched chain lipid (phytol + BCFA). Total branched lipid accumulation was greater in females than males. DKO exacerbated these effects in males as the accumulation of these branched chain lipids reached nearly the same level as females.

3.5. *Scp-2/Scp-x* gene ablation (DKO) differentially alters the composition of hepatic fatty acid species in female vs male phytol-fed mice

Because DKO exacerbated hepatic accumulation of branched-chain lipids in the above phytol-fed mice, it was important to determine whether this also resulted in changes in the total fatty acid (FA) content.

Although hepatic total fatty acid content of control-fed female and male WT mice did not differ, phytol-diet increased that in phytol-fed females but not males (Fig. 3A,B). This increase was quantitatively associated with a large increase in total branched chain fatty acid (BCFA) (Fig. 3C,D).

DKO decreased the hepatic total fatty acid in control-fed females, but not males (Fig. 3A,B). However, this decrease was not associated with any detectable BCFA (Fig. 3C,D). On phytol diet, DKO increased liver total fatty acid content in males (Fig. 3B) but did not further alter liver total fatty acid content in females (Fig. 3A) which masked the small but significant increase in BCFA (Fig. 3C).

Taken together, these data suggested that DKO alone decreased hepatic total fatty acid content in female, but not male mice. Dietary phytol induced hepatic total fatty acid accumulation; an effect exacerbated by *Scp-2/Scp-x* gene ablation, especially in the female mice. Finally, DKO increased the proportion of BCFA among the total fatty acids in phytol-fed males and less so females.

3.6. Scp-2/Scp-x gene ablation (DKO) differentially impacts the sexual dimorphic effect of dietary phytol on hepatic accumulation of individual branched-chain fatty acid (BCFA) species

The possibility that DKO may differentially induce hepatic accumulation of select phytol-derived metabolites, GC/MS was performed as described in Methods to quantitate hepatic content of: i) phytanic acid, produced from phytol in endoplasmic reticulum; ii) pristanic acid and 2,3-pristenic acid, both produced in the peroxisomal matrix [2, 33].

In livers of control-fed female and male WT mice the major phytol metabolite, i.e. phytanic acid, was within the baseline (Fig. 4A,B)— 0.47 ± 0.08 and 1.35 ± 0.2 nmol/mg, respectively. This represented <0.2 % of hepatic total fatty acids (Supplemental Fig. 1A,B). The downstream peroxisomal metabolites of phytanic acid were present at even lower levels in control-fed female and male WT mice (Fig. 4)— 0.11 ± 0.02 and 0.09 ± 0.03 nmol/mg for pristanic acid (Fig. 4C,D); 1.7 ± 0.2 nmol/mg and not detectable for 2,3-pristenic acid (Fig. 4E,F). This represented <0.01 and $<0.2\%$ of hepatic total fatty acids, respectively, in female and male WT mice (Supplemental Fig. 1). Thus, livers of control-fed female WT mice accumulated low but more downstream peroxisomal metabolites of phytanic acid than their male counterparts.

In WT mice, there was phytol-diet induced sex-dependent hepatic accumulation of measured phytol metabolites. Livers of phytol-fed WT females accumulated primarily high levels of phytanic acid (405 ± 19 nmol/mg) and less so pristanic acid (1.3 ± 0.2 nmol/mg) (Fig. 4A,C; Phytol). This represented 860- and 12-fold respectively, more than in livers of control-fed WT females (Fig. 4A,C; Control). There was an associated 5.7-fold reduction in 2,3-pristenic acid (0.3 ± 0.1 nmol/mg) (Fig. 4E; Phytol vs Control). These differences were also evident when expressed on the basis of % composition (Supplemental Fig. 1A,C,and E). In contrast, livers of phytol-fed WT males accumulated as much as 12-fold lower levels of phytanic acid (34 ± 9 nmol/mg) and 4-fold lower levels of pristanic acid (0.3 ± 0.1 nmol/mg) but 3.7-fold higher in 2,3-pristenic acid (1.1 ± 0.2 nmol/mg) (Fig. 4B,D,and F; Phytol). This represented only 25- and 3.5-fold more than in livers of control-fed WT males (Fig. 4B,D; Control) for phytanic acid and pristanic acid while substantially increasing the 2,3-pristenic acid which was not detectable in the male WT control-fed males (Fig. 4F). These differences were also evident when expressed on the basis of % composition (Supplemental Fig. 1B,D,and F). Thus, dietary phytol selectively induced hepatic accumulation of phytanic acid (produced in the endoplasmic reticulum from phytol) in WT females, while inducing accumulation of peroxisomal phytanic acid metabolites to a greater degree in WT males.

DKO decreased hepatic accumulation of phytol metabolites in control-fed female and less so male control-fed mice. In females, DKO decreased liver mass of phytanic acid, pristanic acid, and 2,3-pristenic acid to 0.23 ± 0.08 , 0.05 ± 0.01 , and 0.8 ± 0.2 nmol/mg, respectively, near baseline levels (Fig.4A,C,and E). Based on mass, this was about half the respective levels in control-fed DKO females (Fig. 4A,C, and E; Suppl. Fig 1A,C,and E). When expressed on the basis of % fatty acid composition, the control-fed DKO males also clearly accumulated less phytanic acid, pristanic acid, and 2,3-pristenic acid, than control-fed females the less prevalent metabolites (Suppl. Fig 1B,D,and F vs Suppl. Fig. 1A,C,and E).

Finally, in the context of dietary phytol DKO increased the accumulation of phytol metabolites such that overall levels in females and males did not differ as much as in phytol-fed WT counterparts. Livers of phytol-fed DKO females accumulated highest levels of phytanic acid (491 ± 39 nmol/mg), pristanic acid (0.09 ± 0.01 nmol/mg), and 2,3-pristanic acid (0.7 ± 0.1 nmol/mg), respectively (Fig. 4A,C, and E; DKO Phytol). This represented 2134-, 2-, and 0-fold respectively, more than in livers of control-fed DKO females (Fig. 4A,C, and E; Phytol vs Control). Differences in the less prevalent metabolites were less evident when expressed on the basis of % composition (Supplemental Fig. 1A,C, and E). Livers of phytol-fed DKO males accumulated phytanic acid (330 ± 70 nmol/mg), pristanic acid (0.8 ± 0.2 nmol/mg), and 2,3-pristanic acid (1.2 ± 0.5 nmol/mg to detectable) (Fig. 4B,D, and F; DKO Phytol). When expressed on the basis of % fatty acid composition, the phytol-fed DKO males accumulated more phytanic acid, but not the less prevalent metabolites (Supplemental Fig. 1B,D, and F).

In summary, phytol-diet primarily induced hepatic accumulation of the endoplasmic reticulum metabolite of phytol (phytanic acid), while those of the peroxisomal metabolites (pristanic acid, 2,3-pristanic acid) accumulated to much lesser degree in female WT mice and even less so WT males. DKO significantly exacerbated phytol-induced hepatic accumulation of these metabolites (phytanic acid \gg pristanic and 2,3-pristanic acids) not only in females but also males. Thus, DKO tended to diminish or mitigate the sex-differences in dietary phytol-induced hepatic accumulation of BCFA metabolites of phytol.

3.7. Effect of sex on hepatic total fatty acid mass: role of dietary phytol and SCP-2/SCP-x gene ablation (DKO)

The structure and packing of lipids containing branched-chain fatty acids (BCFA) differs markedly (i.e. more fluid) from lipids with straight-chain fatty acids (LCFA) [36–40]. Therefore, the possibility that the observed accumulation of BCFA in phytol-fed WT and KO mice might elicit compensatory changes in the composition of the LCFA was examined by GC/MS as described in Methods.

The distribution of individual LCFA species of liver lipids differs little between control-fed female and male WT mice, regardless of whether LCFA composition was expressed on the basis of mass (Supplemental Table 2 vs 4) or % (Supplemental Table 3 vs 5). Likewise, the degree of LCFA unsaturation (total saturated, total unsaturated, monounsaturated, polyunsaturated) differed little between males and females, regardless whether expressed on the basis of mass (Fig. 5) or % (Supplemental Fig. 2).

Since phytol-fed WT females accumulated more hepatic total fatty acid mass (Fig. 3A,B) than could be accounted for by increased BCFA mass (Fig. 3C,D), not surprisingly the mass contents of individual LCFA species were altered (Supplemental Table 2). Phytol-fed WT females had much more saturated LCFA (Fig. 5A), primarily C14:0 and C18:0, regardless of whether expressed as mass (Supplemental Table 2) or % (Supplemental Table 3). Conversely, phytol-fed WT females had less unsaturated LCFA, primarily C18:1, C20:4, and C22:6, regardless of whether expressed on the basis of mass (Fig. 5C) or % (Supplemental Fig 2C). Similar observations were made for monounsaturated LCFA, i.e. MUFA (Fig. 5E; Supplemental Fig 2E) and polyunsaturated LCFA, i.e. PUFA (Fig. 5G; Supplemental Fig

2G). In contrast, phytol-diet had much less impact on hepatic LCFA distribution in WT males when expressed on the basis of either mass (Fig. 5B,D,F, and H) or % (Supplemental Fig 2B,D,F, and H). Thus, phytol-diet decreased the proportion of all unsaturated LCFA classes in female but not male WT mice.

The preferential DKO-induced decrease in total fatty acid mass in livers of control-fed females, but not males (Fig. 3C vs D) was LCFA species selective. Liver LCFA of control-fed DKO females exhibited increased mass of saturated LCFA (Fig. 5A, Supplemental Table 2) concomitant with decreased total unsaturated (Fig. 5C, Supplemental Table 2), MUFA (Fig. 5E, Supplemental Table 1), and PUFA (Fig. 5G, Supplemental Table 2). In contrast, in control-fed males DKO had relatively much less impact on either the mass distribution (Fig. 5B,D,F, and H, Supplemental Table 4) or % distribution (Supplemental Tables 4, 5) of hepatic total LCFA species. Thus, DKO selectively increased hepatic content of saturated LCFA, but decreased that of all unsaturated LCFA classes in female but not male control-fed mice.

Overall the hepatic phenotype of individual LCFA species in phytol-fed DKO female mice was very similar to that of phytol-fed WT mice whether expressed on the basis of mass (Fig. 5A,C,E, and G; Supplemental Table 1) or % (Supplemental Fig. 2A,C,E, and G; Supplemental Table 3). However, livers of phytol-fed male DKO mice exhibited increased saturated LCFA concomitant with decreases in all unsaturated LCFA classes regardless whether expressed as mass (Fig. 5B,D,F, and H) or % (Supplemental Fig. 2B,D,F, and H). Thus, overall the hepatic LCFA composition of phytol-fed DKO females was not altered more than that of phytol-fed WT females. However, DKO significantly decreased the proportion of unsaturated to saturated LCFA in males, closer to the levels of those in females.

Taken together, these data showed that the hepatic LCFA composition of female WT mice was much more susceptible than that of WT males to dietary challenge by phytol. Overall DKO did not further alter the proportions of LCFA classes in phytol-fed females, but significantly increased the unsaturated/saturated ratios in males. Thus, phytol-diet induced accumulation of membrane-perturbing BCFA elicited potentially compensatory increases in hepatic LCFA, i.e. increased saturated LCFA and decreased unsaturated LCFA, in WT females, but not males. Likewise, accumulation of BCFA induced by phytol-diet elicited concomitant increased hepatic saturated LCFA but decreased unsaturated LCFA in DKO males.

3.8. Effect of DKO and phytol-diet on sex differences in ratios of hepatic LCFA subclasses

The LCFA subclass distributions were calculated as saturated/unsaturated ratio, PUFA/MUFA ratio, double bond index (DBI), and peroxidizability index as in Methods.

Control-fed WT mice did not differ significantly the ratios of unsaturated/saturated LCFA, PUFA/MUFA, double bond index (DBI), or peroxidizability index between female and male (Fig. 6A,C,E, and G). In contrast, dietary phytol significantly increased the saturated/unsaturated LCFA ratio and concomitantly decreased the DBI and peroxidizability indices in WT females (Fig. 6A, E, and G) but not in WT males (Fig. 6B,F, and H). DKO alone

significantly decreased DBI and peroxidizability indices in control-fed females (Fig. 6E,G) but not males (Fig. 6F,H). Phytol-fed female DKO mice overall exhibited similar ratios of saturated/unsaturated LCFA and PUFA/MUFA, the double bond index (DBI), and peroxidizability index as phytol-fed WT females (Fig. 6A, C,E, and G). In contrast, phytol-fed male DKO mice showed the following: a higher ratio of saturated/unsaturated LCFA (Fig. 6B), a similar ratio of PUFA/MUFA (Fig. 6D), a lower double bond index (DBI) (Fig. 6F), and a lower peroxidizability index (Fig. 6H) as compared to phytol-fed WT males.

Thus, DKO alone selectively altered the DBI and peroxidizability index in females. Phytol-diet alone altered ratios and indices to reflect increased LCFA saturation and decreased peroxidizability. Finally, DKO mice on phytol diet showed increased proportion of saturated LCFA at the expense of unsaturated LCFA, the DBI and peroxidizability index.

4. Discussion

The enzymatic pathway and intracellular localization for metabolism of dietary phytol is increasingly well understood [1–3]. In contrast, much less is known about the role of intracellular proteins responsible for binding/transporting the very poorly aqueous soluble phytol and its metabolites to endoplasmic reticulum, peroxisomes and/or within peroxisomes. A likely candidate is the sterol carrier protein-2/sterol carrier protein-x (*Scp-2/Scp-x*) gene which encodes two proteins (SCP-2 and SCP-x) through alternate transcription sites [9]. SCP-2 is localized at near equal mass distribution between cytosol and peroxisomes, but is >50-fold more concentrated within the peroxisomal matrix [9, 11, 41]. SCP-2 nevertheless has high affinity for downstream phytol metabolites produced in the endoplasmic reticulum and peroxisomal matrix—phytanic acid (Fig. 1) and pristanic acid (Fig. 1) [5, 6]—and even more tightly their respective activated –CoA thioesters [6]. Furthermore, the hepatic mRNA expression of SCP-2 has been reported to be affected by phytol diet dependent upon the degree of saturation of other principal fatty acids in the diet [42]. In contrast SCP-x, the only known enzyme with branched-chain acyl-CoA 3-ketothiolase activity needed for oxidizing BCFA, is exclusively peroxisomal [13, 14]. How SCP-2 mediates its effects on phytol and its metabolites, especially in females, is less clear. The work presented herein provided the following new insights.

4.1 SCP-2 binding affinity to phytol

As shown by NBD-stearic acid displacement assay, SCP-2 binds phytanic acid and pristanic acid with high affinity but has very weak affinity for phytol. Although ANS may bind to a different site in SCP-2 than NBD-stearic acid, an earlier ANS displacement study similarly showed that SCP2 binds phytanic acid but has negligible affinity for phytol [43]. This pattern was also observed with the nuclear receptor RXR α which has 15-fold less affinity of phytol than for phytanic acid [16, 17]. The low affinity of SCP-2 for binding phytol would suggest that, despite the nearly 50% of SCP-2 localized in cytosol [9, 11, 41], SCP-2 does not play a role in facilitating the uptake and/or intracellular transport/targeting of phytol. This is in marked contrast to SCP-2's role in binding another branched-chain alcohol, i.e. cholesterol [34, 44, 45], and facilitating its metabolism by enhancing HDL-cholesterol uptake [46, 47] and cytoplasmic transport/targeting to and for esterification (endoplasmic

reticulum) and oxidation (mitochondria and/or peroxisomes) [48]. While the identity of the hepatic cytosolic protein(s) that might function in phytol binding, uptake, and transport is not known, several possibilities may be considered: i) The even more highly prevalent liver fatty acid binding protein (FABP1) shares overlapping ligand specificity with SCP2, but like SCP2 does not bind phytol [43]; ii) The major hepatic cellular retinol binding protein (CRBP1) binds another lipidic alcohol (retinol) with high affinity K_d of 16 nM [49]. While retinol differs from phytol in having five double bonds and a cyclic methyl terminus, nevertheless retinol shares significant structural similarity with phytol since both are straight-chain, methyl branched, lipidic alcohols. The close relationship between CRBPs and FABPs is suggested by site directed mutagenesis of a single amino acid in the binding site of CRBP II resulting in decreased ability to bind retinol concomitant with gain in palmitic acid binding ability [50].

4.2 The sex-dependent impact of DKO on hepatic accumulation of phytol

Scp-2/Scp-x gene ablation (DKO) markedly impacted the hepatic accumulation of phytol. In male DKO mice, dietary phytol induced marked hepatic accumulation of phytol to near 71 nmol/mg, substantially more than the WT male mice. In contrast, the female DKO mice showed no significant increase over the hepatic phytol accumulation in WT female mice, which already have low hepatic levels of both SCP-2 and SCP-x in comparison to the males [4, 15, 51]. Since phytol itself directly binds and activates PPAR α [52], hepatic expression of multiple genes (including *Scp-2/Scp-x*) in the metabolism of phytol is regulated through the highly expressed nuclear receptor, peroxisome proliferator-activated receptor- α (PPAR α). Interestingly, in 0.5% phytol-fed male *Ppara* gene ablated mice the liver accumulated only low levels of phytol near 1.5 nmol/mg [52]. Thus, livers of phytol-fed male *Ppara* gene ablated mice accumulated approximately 47-fold less phytol as compared to their *Scp-2/Scp-x* gene ablation (DKO) counterparts. Taken together, these findings suggested that the *Scp-2/Scp-x* gene (a target gene of *Ppara*) had a greater impact on hepatic phytol accumulation than PPAR α itself. This difference may be explained in part by the fact that induction of the *Scp-2/Scp-x* is regulated not only by PPAR α but also by other transcription factors [4, 9, 15].

4.3 The involvement of DKO in peroxisomal metabolites of phytol

DKO differentially induced hepatic accumulation of peroxisomal metabolites of dietary phytol in female vs male mice. This was consistent with the fact that SCP-2 binds phytanoyl and pristanoyl-CoA within the peroxisomal matrix [2, 5, 6, 12], directly binds to fatty acid oxidative enzymes within peroxisomes [12], and enhances the activity of the first enzymatic step in peroxisomal α -oxidation of branched-chain fatty acids catalyzed by phytanoyl-CoA hydroxylase [7]. Phytanic acid (major phytol metabolite in liver) levels were markedly increased in response to phytol diet—especially in females. The peroxisomal phytol metabolite (after phytanic acid), detected at the next highest level in phytol-fed WT females was pristanic acid while that in WT males was 2,3-pristenic acid. DKO exacerbated the phytol-diet induced increase in phytanic acid in both sexes and pristanic acid only in males. Phytol's metabolite profile in WT and DKO male mice on the C57BL/6NCr background was qualitatively similar to that of an earlier study of focused only on male WT and DKO mice generated via a different construct strategy (C57BL/6J) [6]. Likewise, quantitatively the

hepatic fold-enrichment of phytanic acid (6-fold) in phytol-fed DKO vs WT male mice was very similar between the two studies. This was somewhat surprising since the earlier study used a 5-10-fold higher amount of phytol in the phytol-diet. Thus, an even higher metabolite accumulation would have been expected as compared to that described herein. While the basis for this conundrum is not known, the latter study [6]: i) used a different mouse genetic background (C57BL/6J vs C57BL/NCr); ii) used a control diet that contained 35-fold higher levels of phytol as well as high levels of dietary phytanic acid (0.02%) which was not detectable in the defined diet used herein; iii) exhibited marked hepatotoxicity due to the 5–10 fold higher dietary phytol [6]. Much less toxicity has been observed at 0.5% dietary phytol [4, 15, 53, 54]. At toxic phytol levels, especially in DKO males, the liver may be less effective in further taking up and metabolizing phytol.

4.4 The role of phytol metabolism on proportion of saturated versus unsaturated straight-chain fatty acids

It was shown for the first time that, concomitant with accumulation of BCFA in hepatic lipids of phytol-fed male DKO mice, the proportion of saturated straight-chain fatty acids (LCFA) increased at the expense of unsaturated LCFA. Incorporation of BCFA such as phytanic acid into membrane phospholipids disturbs membrane phospholipid acyl chain packing by reducing lipid condensation, decreasing bilayer thickness, lowering chain ordering, and increasing fluidity [36–40]. Taken together, these findings would suggest that concomitant increases in hepatic esterified saturated LCFA as well as decreased levels of unsaturated LCFA would contribute to decrease fluidity/increase rigidity, thereby compensating in part for increased fluidity produced by accumulation of BCFA. While the metabolic basis for this potentially compensatory mechanism remains to be elucidated, polyunsaturated LCFA are oxidized primarily in peroxisomes. Furthermore, both SCP-2 and SCP-x facilitate peroxisomal oxidation of LCFA as well as BCFA [14, 55, 56] and SCP-2 binds LCFA and their CoA thioesters [5, 23]. Finally, livers of DKO mice exhibit peroxisomal proliferation, elevated peroxisomal enzymes/activity of fatty acid oxidative enzymes (acyl-CoA oxidase, p-thiolase, m-thiolase), and higher expression of LCFA β -oxidative enzymes (mitochondrial butyryl-CoA dehydrogenase) [6].

4.5 The role of SCP-2 vs FABP1 in hepatic phytol metabolism

A proposed scheme whereby SCP-2, FABP1, and SCP-x mediate hepatic phytol metabolism is shown in Fig. 7. Taken together with findings of an earlier study on phytol metabolism in mice ablated in both *Fabp1* and *Scp-2/Scp-x* genes (TKO) [43], the data presented herein help to resolve the relative contributions of SCP-2 vs FABP1 in hepatic phytol metabolism. As shown herein, ablation of the *Scp-2/Scp-x* gene (DKO) in phytol fed mice significantly increased hepatic accumulation of branched-chain fatty acids about 20% in females (to 500 nmol/mg protein) and nearly 7-fold in males (to about 380 nmol/mg protein). Since *Scp-2/Scp-x* gene ablation (DKO) elicits concomitant upregulation of hepatic FABP1 expression [6, 26, 57], it is unclear whether the increased hepatic phytol accumulation was due to loss of SCP-2/SCP-x or to concomitant upregulation of FABP1. By transporting bound phytanic acid and phytanic acid from the ER to the peroxisome, the increased FABP1 may indirectly increase uptake of phytol. This issue was further resolved in phytol-fed mice ablated in both the *Fabp1* and *Scp-2/Scp-x* genes (TKO) [43]. Ablating both the *Fabp1* and *Scp-2/Scp-x*

genes (TKO) ablated mice increased hepatic accumulation of branched-chain fatty acids similarly as in DKO mice—only about 20% in females (to about 400 nmol/mg protein) and about 7-fold in males (to about 300 nmol/mg protein) fed the same phytol diet. These data taken together showed that in phytol-fed mice the *Scp-2/Scp-x* gene products were primarily responsible for hepatic accumulation of branched-chain fatty acid metabolites.

In summary, these findings along with the hepatic metabolism of dietary phytol were consistent with roles for the *Scp-2/Scp-x* gene products (SCP-2, SCP-x) in intrahepatic metabolism of phytol rather than uptake of phytol into hepatocytes. However, the low affinity of SCP-2 for phytol does not negate a role for cytoplasmic SCP-2 (accounting for nearly half of total SCP-2) in the hepatic uptake of dietary phytanic acid. It is important to note, that in contrast to the defined phytol-free, phytanic acid-free rodent diet used herein, standard rodent chow may contain high levels of phytanic acid as well as phytol [6, 58]. In addition phytanic acid produced from phytol by bovine rumen bacteria represents as much as 2.8% of total fatty acid herein [1]. Phytanic acid accumulates at high levels in bovine meat and milk, especially in cows fed ensilage for several months wherein phytanic acid represents 8% of total LCFA [1]. Studies with transfected cells and cultured primary hepatocytes from *Fabp1* gene ablated mice show that FABP1 enhances phytanic acid uptake and oxidation [59–61]. This would suggest that FABP1 as well as SCP-2 and SCP-x both play important roles in hepatic uptake and metabolism of branched-chain fatty acids. Another important observation of this study was that the *Scp-2/Scp-x* gene is major contributor to the sexual-dimorphic hepatic metabolism of phytol in mice. Finally, the findings described herein with *Scp-2/Scp-x* null mice may potentially be significant to our understanding of the roles of these proteins in human phytol metabolism since human patients genetically deficient in SCP-x (but not SCP-2) exhibited significant deficiencies in peroxisomal oxidation of branched-chain lipids [62, 63].

Supplementary Material

Refer to Web version on PubMed Central for supplementary material.

Acknowledgments

This work was supported in part by the USPHS, National Institutes of Health Grant DK41402 (F.S. and A.B.K.).

Abbreviations

BCFA	branched-chain fatty acids
DKO	<i>Scp-2/Scp-x</i> gene ablated mice
FABP1	liver fatty acid binding protein-1
LKO	<i>Fabp1</i> gene ablated mice
FAME	fatty acid methyl esters
GC	gas chromatography

GC-MS	gas chromatography-mass spectrometry
phytanic acid	3,7,11,15-tetramethylhexadecanoic acid
pristanic acid	2,6,10,14-tetramethylpentadecanoic acid
phytol	3,7,11,15-tetramethylhexadec-2-en-1-ol
PPARα	peroxisome proliferator activated receptor- α
RXR	retinoid X receptor
SCP-2	sterol carrier binding protein
SCP-x	sterol carrier protein-x
WT	wild-type mice

References

- Jansen GA, Wanders RJA. Alpha Oxidation. *Biochim Biophys Acta*. 2006; 1763:1403–1412. [PubMed: 16934890]
- Wanders RJA, Komen J, Ferdinandusse S. Phytanic acid metabolism in health and disease. *Biochim Biophys Acta*. 2011; 1811:498–507. [PubMed: 21683154]
- Van Veldhoven PP. Biochemistry and genetics of inherited disorders of peroxisomal fatty acid metabolism. *J Lipid Res*. 2010; 51:2863–2895. [PubMed: 20558530]
- Atshaves BP, McIntosh AL, Landrock D, Payne HR, Mackie J, Maeda N, Ball JM, Schroeder F, Kier AB. Effect of SCP-x gene ablation on branched-chain fatty acid metabolism. *Am J Physiol*. 2007; 292:939–951.
- Frolov A, Miller K, Billheimer JT, Cho TC, Schroeder F. Lipid specificity and location of the sterol carrier protein-2 fatty acid binding site: A fluorescence displacement and energy transfer study. *Lipids*. 1997; 32:1201–1209. [PubMed: 9397406]
- Seedorf U, Raabe M, Ellinghaus P, Kannenberg F, Fobker M, Engel T, Denis S, Wouters F, Wirtz KWA, Wanders RJA, Maeda N, Assmann G. Defective peroxisomal catabolism of branched fatty acyl coenzyme A in mice lacking the sterol carrier protein-2/sterol carrier protein-x gene function. *Genes and Development*. 1998; 12:1189–1201. [PubMed: 9553048]
- Mukherji M, Kershaw NJ, Schofield CJ, Wierzbicki AS, Lloyd MD. Utilization of sterol carrier protein-2 by phytanoyl-CoA 2-hydroxylase in the peroxisomal alpha oxidation of phytanic acid. *Chemistry and Biology*. 2002; 9:597–605. [PubMed: 12031666]
- Mukherji M, Schofield CJ, Wierzbicki AS, Jansen GA, Wanders RJA, Lloyd MD. The chemical biology of branched-chain lipid metabolism. *Prog Lipid Res*. 2003; 42:359–376. [PubMed: 12814641]
- Gallegos AM, Atshaves BP, Storey SM, Starodub O, Petrescu AD, Huang H, McIntosh A, Martin G, Chao H, Kier AB, Schroeder F. Gene structure, intracellular localization, and functional roles of sterol carrier protein-2. *Prog Lipid Res*. 2001; 40:498–563. [PubMed: 11591437]
- Martin GG, Hostetler HA, McIntosh AL, Tichy SE, Williams BJ, Russell DH, Berg JM, Spencer TA, Ball JA, Kier AB, Schroeder F. Structure and function of the sterol carrier protein-2 (SCP-2) N-terminal pre-sequence. *Biochem*. 2008; 47:5915–5934. [PubMed: 18465878]
- Keller GA, Scallen TJ, Clarke D, Maher PA, Krisans SK, Singer SJ. Subcellular localization of sterol carrier protein-2 in rat hepatocytes: its primary localization to peroxisomes. *J Cell Biol*. 1989; 108:1353–1361. [PubMed: 2925789]
- Wouters F, Bastiaens PI, Wirtz KW, Jovin TM. FRET microscopy demonstrates molecular association of non-specific lipid transfer protein (nsL-TP) with fatty acid oxidation enzymes. *EMBO J*. 1998; 17:7179–7189. [PubMed: 9857175]

13. Seedorf U, Brysch P, Engel T, Schrage K, Assmann G. Sterol carrier protein X is peroxisomal 3-oxoacyl coenzyme A thiolase with intrinsic sterol carrier and lipid transfer activity. *J Biol Chem.* 1994; 269:21277–21283. [PubMed: 8063752]
14. Antonenkov VD, Van Veldhoven PP, Waelkens E, Mannaerts GP. Substrate specificities of 3-oxoacyl-CoA thiolase A and sterol carrier protein 2/3-oxoacyl-CoA thiolase purified from normal rat liver peroxisomes. *J Biol Chem.* 1997; 272:26023–26031. [PubMed: 9325339]
15. Atshaves BP, Payne HR, McIntosh AL, Tichy SE, Russell D, Kier AB, Schroeder F. Sexually dimorphic metabolism of branched chain lipids in C57BL/6J mice. *J Lipid Res.* 2004; 45:812–830. [PubMed: 14993239]
16. Kitareewan S, Burka LT, Tomer KB, Parker CE, Deterding LJ, Stevens RD, Forman BM, Mais DE, Heyman RA, McMorris T, Weinberger C. Phytol metabolites are circulating dietary factors that activate the nuclear receptor RXR. *Mol Biol Cell.* 1996; 7:1153–1166. [PubMed: 8856661]
17. Lemotte PK, Keidel S, Apfel CM. Phytanic acid is a retinoid X receptor ligand. *Eur J Biochem.* 1996; 236:328–333. [PubMed: 8617282]
18. Wolfrum C, Ellinghaus P, Fobker M, Seedorf U, Assmann G, Borchers T, Spener F. Phytanic acid is ligand and transcriptional activator of murine liver fatty acid binding protein. *J Lipid Res.* 1999; 40:708–714. [PubMed: 10191295]
19. Zomer AWM, van der Burg B, Jansen GA, Wanders RJA, Poll-The BT, van der Saag PT. Pristanic acid and phytanic acid: naturally occurring ligands for the nuclear receptor peroxisome proliferator activated receptor alpha. *J Lipid Res.* 2000; 41:1801–1807. [PubMed: 11060349]
20. Adida A, Spener F. Intracellular lipid binding proteins and nuclear receptors involved in branched-chain fatty acid signaling. *Prost Leukot Essen Fatty Acids.* 2002; 67:91–98.
21. Hostetler HA, Kier AB, Schroeder F. Very-long-chain and branched-chain fatty acyl CoAs are high affinity ligands for the peroxisome proliferator-activated receptor alpha (PPARalpha). *Biochemistry.* 2006; 45:7669–7681. [PubMed: 16768463]
22. Finck BN, Bernal-Mizrachi C, Han DH, Coleman T, Sambandam N, LaRiviere LL, Holloszy JO, Semenkovich CF, Kelly DP. A potential link between muscle peroxisome proliferator activated receptor alpha signaling and obesity related diabetes. *Cell Metabolism.* 2005; 1:133–144. [PubMed: 16054054]
23. Frolov A, Cho TH, Billheimer JT, Schroeder F. Sterol carrier protein-2, a new fatty acyl coenzyme A-binding protein. *J Biol Chem.* 1996; 271:31878–31884. [PubMed: 8943231]
24. Hillard, CJ., Huang, H., Vogt, CD., Rodrigues, BE., Neumann, TS., Sem, DS., Schroeder, F., Cunningham, CW. Endocannabinoid Transport Proteins: Discovery of Tools to Study Sterol Carrier Protein-2. In: Patricia, VE., Reggio, H., editors. *Methods In Enzymology: Endocannabinoid Transport Proteins.* Academic Press imprint of Elsevier; Cambridge, MA, USA: 2017. p. 99-122.
25. Schroeder F, Myers-Payne SC, Billheimer JT, Wood WG. Probing the ligand binding sites of fatty acid and sterol carrier proteins: effects of ethanol. *Biochemistry.* 1995; 34:11919–11927. [PubMed: 7547928]
26. Atshaves BP, McIntosh AL, Payne HR, Gallegos AM, Landrock K, Maeda N, Kier AB, Schroeder F. Sterol carrier protein-2/sterol carrier protein-x gene ablation alters lipid raft domains in primary cultured mouse hepatocytes. *J Lipid Res.* 2007; 48:2193–2211. [PubMed: 17609524]
27. Thigpen JE, Setchell KD, Ahlmark KB, Kocklear J, Spahr T, Caviness GF, Goelz MF, Haseman JK, Newbold RR, Forsythe DB. Phytoestrogen content of purified, open- and closed-formula laboratory animal diets. *Lab An Science.* 1999; 49:530–536.
28. Thigpen JE, Setchell KD, Goelz MF, Forsythe DB. The phytoestrogen content of rodent diets. *Environ Health Persp.* 1999; 107:A182–A183.
29. Hara A, Radin NS. Lipid extraction of tissues with a low toxicity solvent. *Anal Biochem.* 1978; 90:420–426. [PubMed: 727482]
30. Jefferson JR, Slotte JP, Nemezc G, Pastuszyn A, Scallen TJ, Schroeder F. Intracellular sterol distribution in transfected mouse L-cell fibroblasts expressing rat liver fatty acid binding protein. *J Biol Chem.* 1991; 266:5486–5496. [PubMed: 2005092]

31. Bradford M. A rapid and sensitive method for the quantitation of microgram quantities of protein utilizing the principle of protein dye binding. *Anal Biochem.* 1976; 72:248–254. [PubMed: 942051]
32. Mocking RJT, Assies J, Lok A, Ruhe HG, Koeter MWJ, Visser I, Bockting CLH, Schene AH. Statistical methodological issues in handling of fatty acid data: percentage or concentration, imputation, and indices. *Lipids.* 2012; 47:541–547. [PubMed: 22446846]
33. Gloerich J, van der Brink DM, Ruiten JPN, van Vlies N, Vaz FM, Wanders RJA, Ferdinandusse S. Metabolism of phytol to phytanic acid in the mouse, and the role of PPARalpha in its regulation. *J Lipid Res.* 2007; 48:77–85. [PubMed: 17015885]
34. Stolowich NJ, Frolov A, Petrescu AD, Scott AI, Billheimer JT, Schroeder F. Holosterol carrier protein-2: ¹³C-NMR investigation of cholesterol and fatty acid binding sites. *J Biol Chem.* 1999; 274:35425–35433. [PubMed: 10585412]
35. Avdulov NA, Chochina SV, Igbavboa U, Warden CH, Schroeder F, Wood WG. Lipid binding to sterol carrier protein-2 is inhibited by ethanol. *Biochim Biophys Acta.* 1999; 1437:37–45. [PubMed: 9931423]
36. Cushley RJ, Forrest BJ. Structure and stability of vitamin E-lecithin and phytanic acid-lecithin bilayers studies by ¹³C and ³¹P NMR. *Can J Chem.* 1977; 55:220–226.
37. Young SP, Johnson AW, Muller DPR. Effects of phytanic acid on the vitamin E status, lipid composition, and physical properties of retinal membranes: implications for adult Refsum disease. *Clinical Science.* 2001; 101:697–705. [PubMed: 11724659]
38. Schonfeld P, Struy H. Refsum disease diagnostic marker phytanic acid alters the physical state of membrane proteins of liver mitochondria. *FEBS Lett.* 1999; 457:179–183. [PubMed: 10471774]
39. Fukuzawa K, Chida H, Suzuki A. Fluorescence depolarization studies of phase transition and fluidity in lecithin liposomes containing alpha-tocopherol. *J Nutr Sci Vitaminol.* 1980; 26:427–434. [PubMed: 6894310]
40. Schwarz D, Kisselev P, Wessel R, Pisch S, Bornscheuer U, Schmid RD. Possible involvement of nonbilayer lipids in the stimulation of the activity of cytochrome P450SCC (CYP11A1) and its propensity to induce vesicle aggregation. *Chem Phys Lipids.* 1997; 85:91–99. [PubMed: 9138891]
41. Schroeder F, Frolov A, Starodub O, Russell W, Atshaves BP, Petrescu AD, Huang H, Gallegos A, McIntosh A, Tahotna D, Russell D, Billheimer JT, Baum CL, Kier AB. Pro-sterol carrier protein-2: role of the N-terminal presequence in structure, function, and peroxisomal targeting. *J Biol Chem.* 2000; 275:25547–25555. [PubMed: 10833510]
42. Hashimoto T, Shimizu N, Kimura T, Takahashi Y, Ide T. Polyunsaturated fats attenuate dietary phytol-induced increase in hepatic fatty acid oxidation in mice. *J Nutr.* 2006; 136:882–886. [PubMed: 16549445]
43. Storey SM, Huang H, McIntosh AL, Martin GG, Kier AB, Schroeder F. Impact of Fabp1/SCP-2/SCP-x gene ablation (TKO) on hepatic phytol metabolism. *J Lipid Res.* 2017; 58:1153–1165. [PubMed: 28411199]
44. Martin GG, Atshaves BP, Huang H, McIntosh AL, Williams BW, Pai PJ, Russell DH, Kier AB, Schroeder F. Hepatic phenotype of liver fatty acid binding protein (L-FABP) gene ablated mice. *Am J Physiol.* 2009; 297:G1053–G1065.
45. Stolowich NJ, Petrescu AD, Huang H, Martin G, Scott AI, Schroeder F. Sterol carrier protein-2: structure reveals function. *Cell Mol Life Sci.* 2002; 59:193–212. [PubMed: 11915938]
46. Moncecchi DM, Murphy EJ, Prows DR, Schroeder F. Sterol carrier protein-2 expression in mouse L-cell fibroblasts alters cholesterol uptake. *Biochim Biophys Acta.* 1996; 1302:110–116. [PubMed: 8695660]
47. Storey SM, McIntosh AL, Huang H, Martin GG, Landrock KK, Landrock D, Payne HR, Kier AB, Schroeder F. Intracellular cholesterol binding proteins enhance HDL-mediated cholesterol uptake in cultured primary mouse hepatocytes. *Am J Physiol Gastrointest and Liver Phys.* 2012; 302:G824–G839.
48. Murphy EJ, Schroeder F. Sterol carrier protein-2 mediated cholesterol esterification in transfected L-cell fibroblasts. *Biochim Biophys Acta.* 1997; 1345:283–292. [PubMed: 9150248]
49. Ong DE, Chytil F. Cellular retinol binding protein from rat liver. Purification and characterization. *J Biol Chem.* 1978; 253:828–832. [PubMed: 563865]

50. Cheng L, Qian SJ, Rothschild C, d'Avignon A, Lefkowitz JB, Gordon JI, Li E. Alteration of the binding specificity of cellular retinol-binding protein II by site-directed mutagenesis. *J Biol Chem.* 1991; 266:24404–24412. [PubMed: 1761542]
51. Klipsic D, Landrock D, Martin GG, McIntosh AL, Landrock KK, Mackie JT, Schroeder F, Kier AB. Impact of SCP-2/SCP-x gene ablation and dietary cholesterol on hepatic lipid accumulation. *Am J Physiol Gastrointest and Liver Phys.* 2015; 309:G387–G399.
52. Goto T, Takahashi N, Kato S, Egawa K, Ebisu S, Moriyama T, Fushiki T, Kawada T. Phytol directly activates peroxisome proliferator activated receptor- α (PPAR α) and regulates gene expression involved in lipid metabolism in PPAR α -expressing HepG2 hepatocytes. *Biochem Biophys Res Commun.* 2005; 337:440–445. [PubMed: 16202384]
53. Atshaves BP, McIntosh AL, Payne HR, Mackie J, Kier AB, Schroeder F. Effect of branched-chain fatty acid on lipid dynamics in mice lacking liver fatty acid binding protein gene. *Am J Physiol.* 2005; 288:C543–C558.
54. Mackie JT, Atshaves BP, Payne HR, McIntosh AL, Schroeder F, Kier AB. Phytol-induced hepatotoxicity in mice. *Toxicol Pathol.* 2009; 37:201–208. [PubMed: 19188468]
55. Atshaves BP, Storey SM, Schroeder F. Sterol carrier protein-2/sterol carrier protein-x expression differentially alters fatty acid metabolism in L-cell fibroblasts. *J Lipid Res.* 2003; 44:1751–1762. [PubMed: 12810824]
56. Wanders RJA, Denis S, Wouters F, Wirtz KWA, Seedorf U. Sterol carrier Protein X (SCPx) is a peroxisomal branched-chain β -ketothiolase specifically reacting with 3-Oxo-pristanoyl-CoA: A new, unique role for SCPx in branched-chain fatty acid metabolism in peroxisomes. *Biochem Biophys Res Commun.* 1997; 236:565–569. [PubMed: 9245689]
57. Fuchs M, Hafer A, Muench C, Kannenberg F, Teichmann S, Scheibner J, Stange EF, Seedorf U. Disruption of the sterol carrier protein 2 gene in mice impairs biliary lipid and hepatic cholesterol metabolism. *J Biol Chem.* 2001; 276:48058–48065. [PubMed: 11673458]
58. Steinberg D, Avigan J, Mize C, Baxter JH, Cammermeyer J, Fales HM, Highet PF. Effects of dietary phytol and phytanic acid in animals. *J Lipid Res.* 1966; 7:684–691. [PubMed: 4165840]
59. Atshaves BP, Storey SM, Petrescu AD, Greenberg CC, Lyuksyutova OI, Smith R, Schroeder F. Expression of fatty acid binding proteins inhibits lipid accumulation and alters toxicity in L-cell fibroblasts. *Am J Physiol.* 2002; 283:C688–C703.
60. Atshaves BP, Storey S, Huang H, Schroeder F. Liver fatty acid binding protein expression enhances branched-chain fatty acid metabolism. *Mol Cell Biochem.* 2004; 259:115–129. [PubMed: 15124915]
61. Atshaves BP, McIntosh AL, Lyuksyutova OI, Zipfel WR, Webb WW, Schroeder F. Liver fatty acid binding protein gene ablation inhibits branched-chain fatty acid metabolism in cultured primary hepatocytes. *J Biol Chem.* 2004; 279:30954–30965. [PubMed: 15155724]
62. Ferdinandusse S, Denis S, van Berkel E, Dacremont G, Wanders RJ. Peroxisomal fatty acid oxidation disorders and 58 kDa sterol carrier protein-x (SCPx): activity measurements in liver and fibroblasts using a newly developed method. *J Lipid Res.* 2000; 41:336–342. [PubMed: 10706581]
63. Ferdinandusse S, Kostopoulos P, Denis S, Rusch R, Overmars H, Dillman U, Reith W, Haas D, Wanders RJA, Duran M, Marziniak M. Mutations in the gene encoding peroxisomal sterol carrier protein X (SCPx) cause leukoencephalopathy with dystonia and motor neuropathy. *Am J Hum Genet.* 2006; 78:1046–1052. [PubMed: 16685654]
64. Shibata H, Ochiai H, Kawashima T, Okamoto T, Inamura I. Preparation and properties of the water-soluble chlorophyll-bovine serum albumin complexes. *Biochim Biophys Acta.* 2017; 852:175–182.
65. Schroeder F, McIntosh AL, Martin GG, Huang H, Landrock D, Chung S, Landrock KK, Dangott LJ, Li S, Kaczocha M, Murphy EJ, Atshaves BP, Kier AB. Fatty acid binding protein-1 (FABP1) and the human FABP1 T94A variant: Roles in the endocannabinoid system and dyslipidemias. *Lipids.* 2016; 51:655–676. [PubMed: 27117865]
66. McArthur MJ, Atshaves BP, Frolov A, Foxworth WD, Kier AB, Schroeder F. Cellular uptake and intracellular trafficking of long chain fatty acids. *J Lipid Res.* 1999; 40:1371–1383. [PubMed: 10428973]

67. Antonenkov VD, Sormunen RT, Ohlmeier S, Amery L, Fransen M. Localization of a portion of the liver isoform of fatty acid binding protein (L-FABP) to peroxisomes. *Biochem J.* 2006; 394:475–484. [PubMed: 16262600]
68. Seedorf U, Ellinghaus P, Nofer JR. Sterol carrier protein-2. *Biochim Biophys Acta.* 2000; 1486:45–54. [PubMed: 10856712]
69. Frolov A, Cho TH, Murphy EJ, Schroeder F. Isoforms of rat liver fatty acid binding protein differ in structure and affinity for fatty acids and fatty acyl CoAs. *Biochemistry.* 1997; 36:6545–6555. [PubMed: 9174372]
70. Murphy EJ, Edmondson RD, Russell DH, Colles SM, Schroeder F. Isolation and characterization of two distinct forms of liver fatty acid binding protein from the rat. *Biochim Biophys Acta.* 1999; 1436:413–425. [PubMed: 9989272]
71. Richieri GV, Ogata RT, Kleinfeld AM. Equilibrium constants for the binding of fatty acids with fatty acid binding proteins from adipocyte, intestine, heart, and liver measured with the fluorescent probe ADIFAB. *J Biol Chem.* 1994; 269:23918–23930. [PubMed: 7929039]
72. Schroeder F, Jolly CA, Cho TH, Frolov AA. Fatty acid binding protein isoforms: structure and function. *Chem Phys Lipids.* 1998; 92:1–25. [PubMed: 9631535]

HIGHLIGHTS

SCP-2 bound phytanic acid but not the precursor phytol.

Dietary phytol induces liver accumulation of phytol and branched-chain metabolites.

Hepatic accumulation of phytol as well as BCFA is greater in wild-type (WT) females.

Scp-2/Scp-x gene ablation (DKO) exacerbates phytol and BCFA accumulation.

Dietary phytol feeding changes proportion of saturated to unsaturated LCFAs.

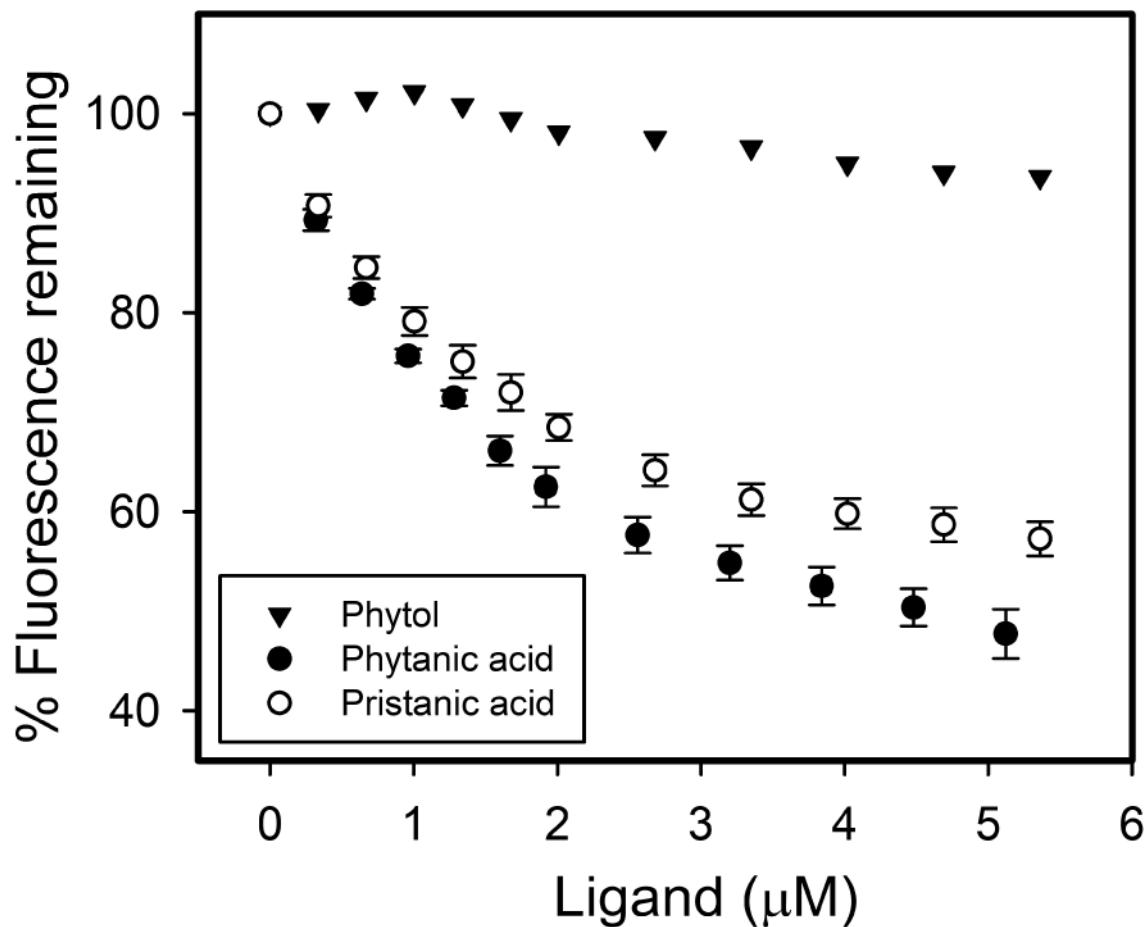


Fig. 1. Binding of phytol and phytol metabolites to SCP-2: NBD-stearic acid displacement assay SCP-2 (500nM) with bound NBD-stearic acid (500 nM) in 10 mM phosphate buffer at pH = 7.4 was titrated with increasing amount of phytol (triangle), phytanic acid (closed circle), or pristanic acid (open circle). NBD-stearic acid fluorescence remaining was measured at the emission maximum (527nm) by scanning emission spectra over the wavelength range of 515–600 nm with 490nm excitation as described in Methods. Values represent average % NBD-stearic acid fluorescence remaining \pm standard error, (n=5), except for phytol (n=1, due to lack of displacement).

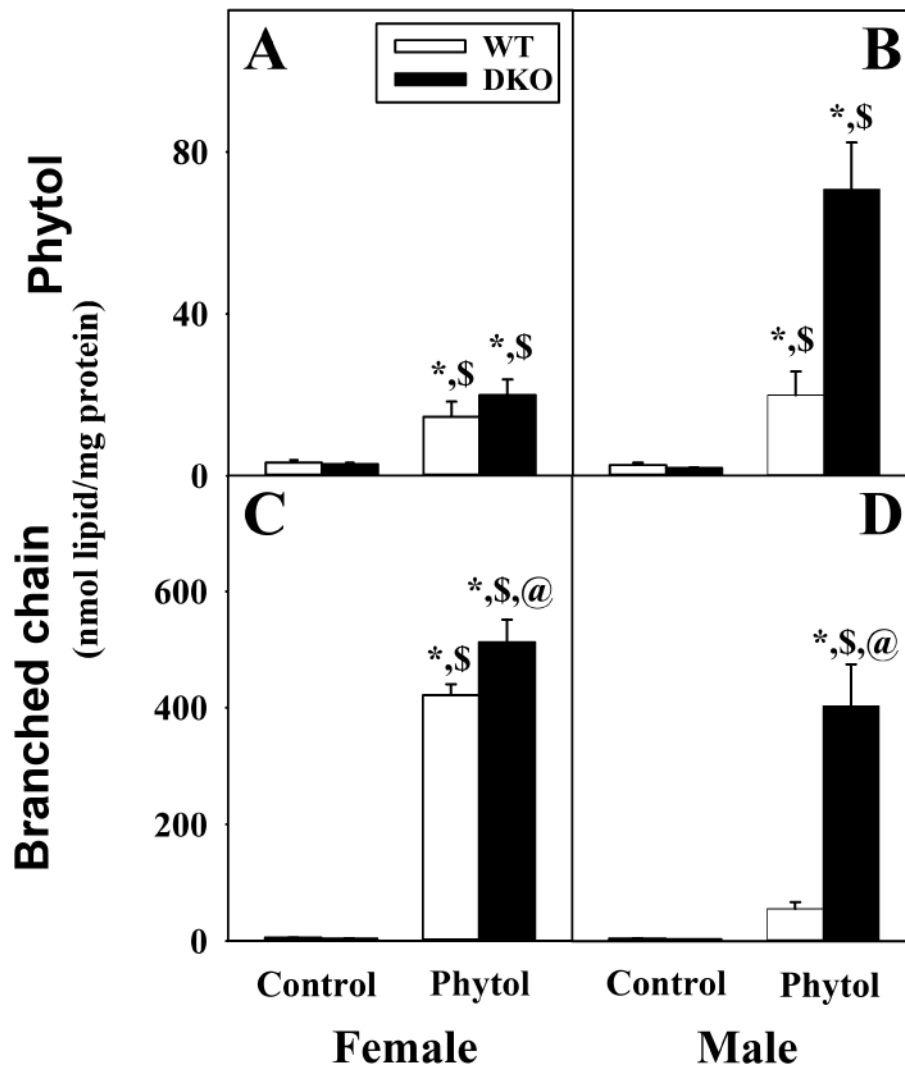


Fig. 2. Sexual dimorphic accumulation of dietary phytol in livers of WT and DKO mice
Phytol (A, B) and total branched-chain lipid, i.e. phytol + branched-chain fatty acids (C,D) content in livers of female (A, C) and male (B, D) wild-type (WT) (white bars) and *Scp-2/Scp-x* null (double knockout; DKO) (black bars) mice fed control or 0.5% phytol-supplemented diet. Values represent average nmol lipid/mg total liver protein \pm standard error (n=4–7); * = P 0.05 compared to WT Control; \$ = P 0.05 compared to DKO Control; @ = P 0.05 compared to WT Phytol.

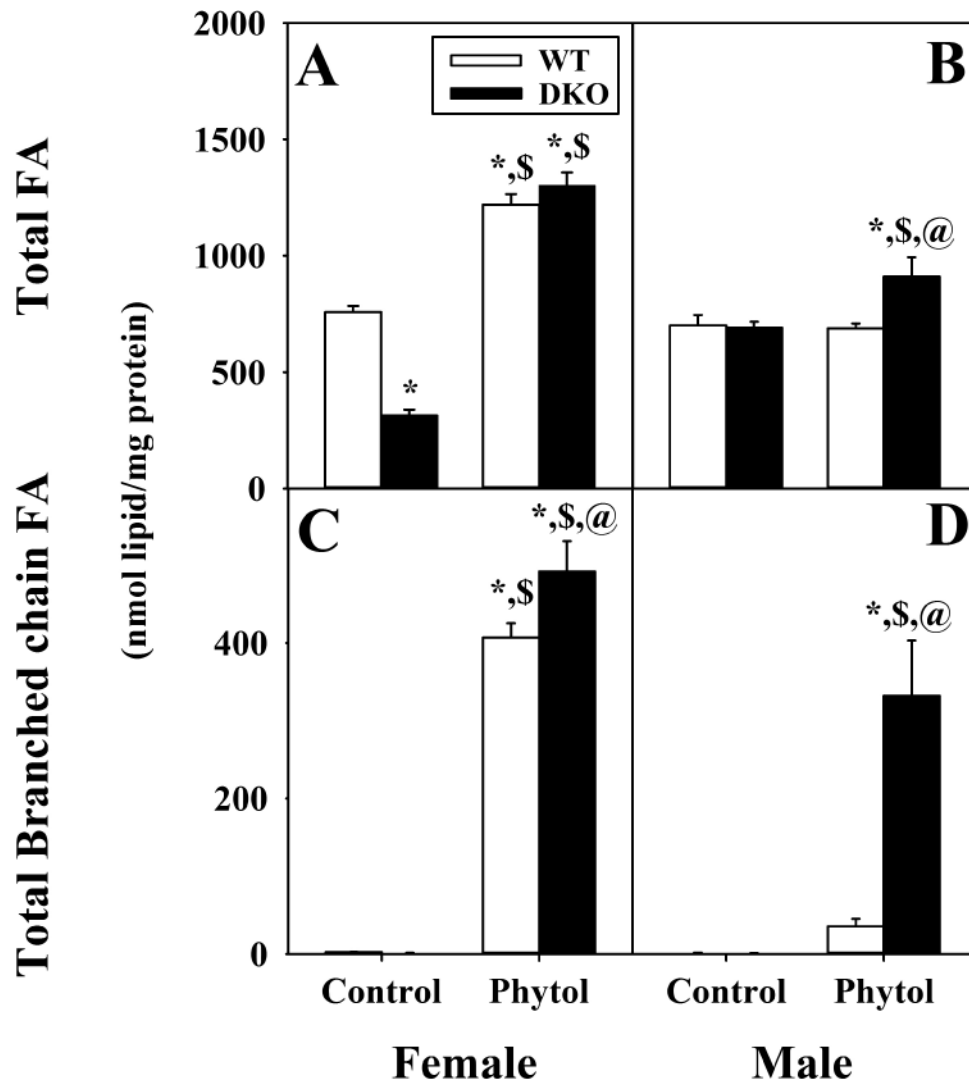


Fig. 3. Impact of dietary phytol and DKO on hepatic content of total fatty acid and branched chain fatty acids (BCFA) in female and male mice
 Total fatty acids (FA) (A,B) and total branched chain fatty acid (BCFA) (C,D) from livers of female (A, C) and male (B, D) wild-type (WT) (white bars) and *Scp-2/Scp-x* null (double knockout; DKO) (black bars) mice fed control or 0.5% phytol-supplemented diet. Values represent average nmol lipid/mg total liver protein \pm standard error (n=4-7); * = P < 0.05 compared to WT Control; \$ = P < 0.05 compared to DKO Control; @ = P < 0.05 compared to WT Phytol.

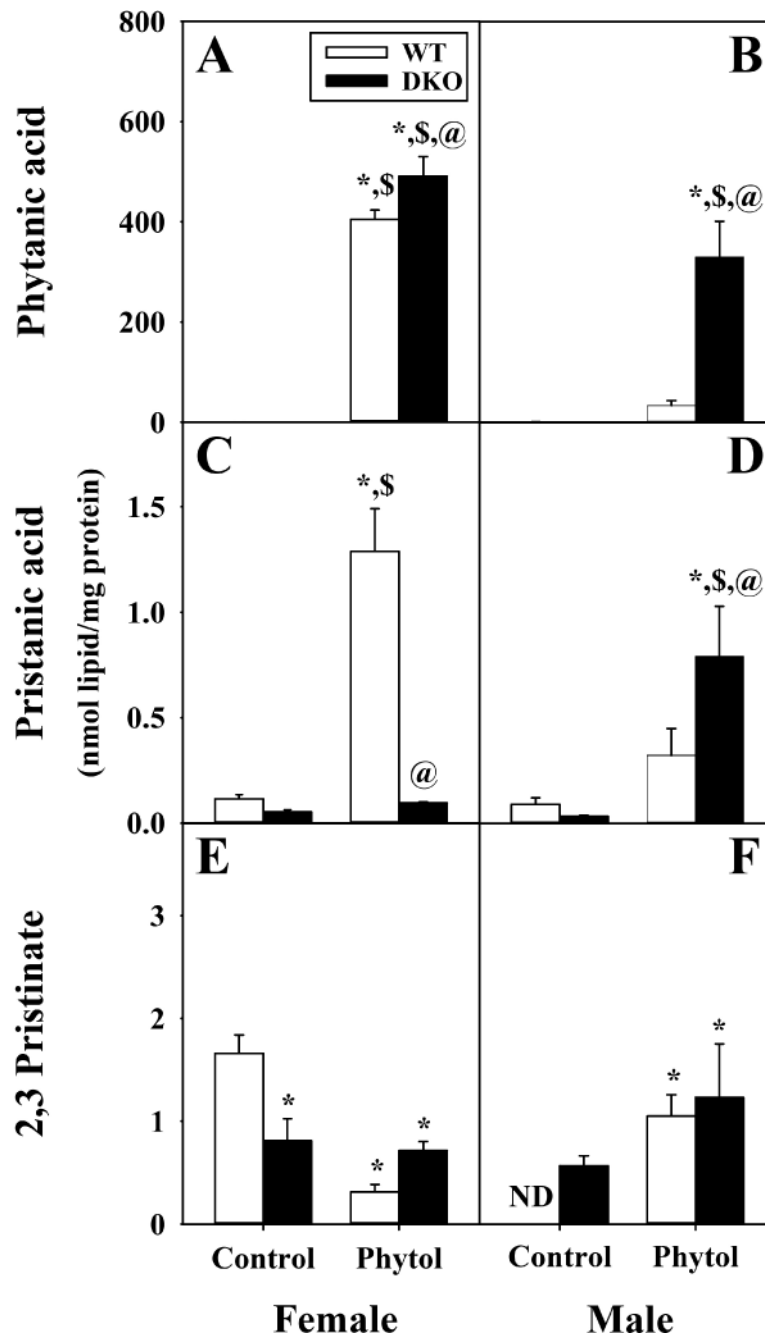


Fig. 4. DKO differentially induces hepatic accumulation of select branched-chain fatty acids (BCFA) in response to phytol-diet
Phytanic acid (A, B), pristanic acid (C, D), and 2,3-pristinate (E, F) from livers of female (A, C, E) and male (B, D, F) wild-type (WT) (white bars) and *Scp-2/Scp-x* null (double knockout; DKO) (black bars) mice fed control or 0.5% phytol-supplemented diet. For each BCFA species, values represent average nmol/mg total liver protein \pm standard error (n=4–8); ND = not detected; * = $P < 0.05$ compared to WT Control; \$ = $P < 0.05$ compared to DKO Control; @ = $P < 0.05$ compared to WT Phytol.

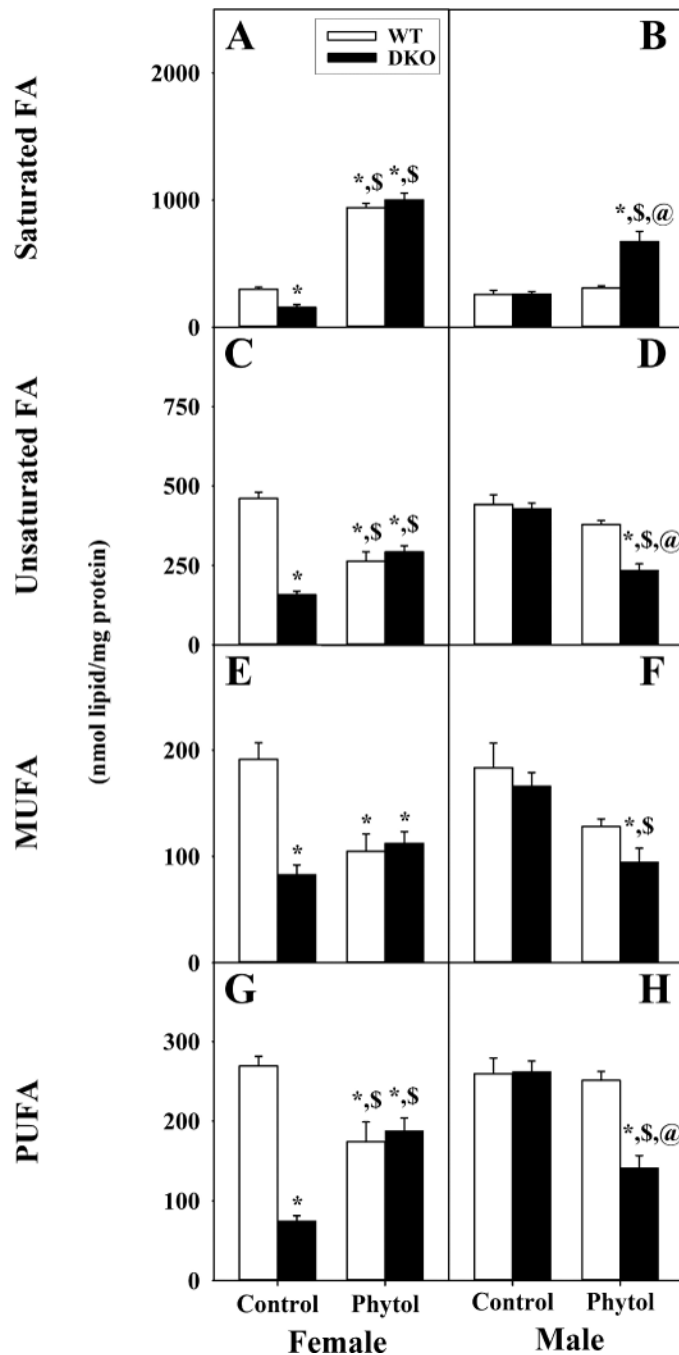


Fig. 5. Sex-dependent impact of DKO and dietary phytol on hepatic accumulation of straight chain fatty acid (LCFA) subclasses (saturated, unsaturated, MUFA, PUFA) in response to dietary phytol

Saturated fatty acids (FA) (A, B), unsaturated FA (C, D), monounsaturated FA (MUFA) (E, F), and polyunsaturated FA (PUFA) (G, H) from livers of female (A, C, E, G) and male (B, D, F, H) wild-type (WT) (white bars) and *Scp-2/Scp-x* null (double knockout; DKO) (black bars) mice fed control or 0.5% phytol-supplemented diet. Values represent average mass of each class of LCFA (nmol/mg total liver protein) \pm standard error (n=4–6); * = P < 0.05

compared to WT Control; \$ = P 0.05 compared to DKO Control; @ = P 0.05 compared to WT Phytol.

Author Manuscript

Author Manuscript

Author Manuscript

Author Manuscript

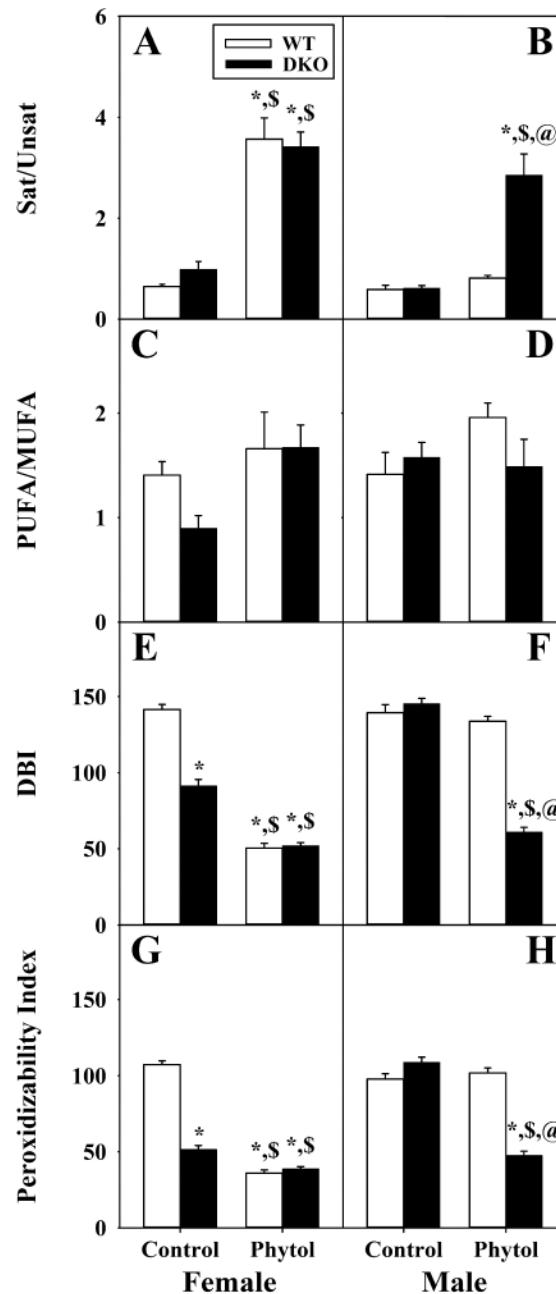


Fig. 6. DKO alters the ratios and indices of straight-chain fatty acid (LCFA) subclasses in livers of phytol-fed mice

Ratios of saturated FA to unsaturated FA (Sat/Unsaturated) (A, B) and polyunsaturated FA to monounsaturated FA (PUFA/MUFA) (C, D) were calculated using the corresponding FA subgroup values from livers of female (A, C) and male (B, D) wild-type (WT) (white bars) and *Scp-2/Scp-x* null (double knockout; DKO) (black bars) mice fed control or 0.5% phytol-supplemented diet. Double bond indexes (DBI) and Peroxidizability indexes were calculated as described in Methods and are presented in the same format. Values represent average ratio (or index) \pm standard error ($n=4-6$); * = $P < 0.05$ compared to WT Control; \$ = $P < 0.05$ compared to DKO Control; @ = $P < 0.05$ compared to WT Phytol.

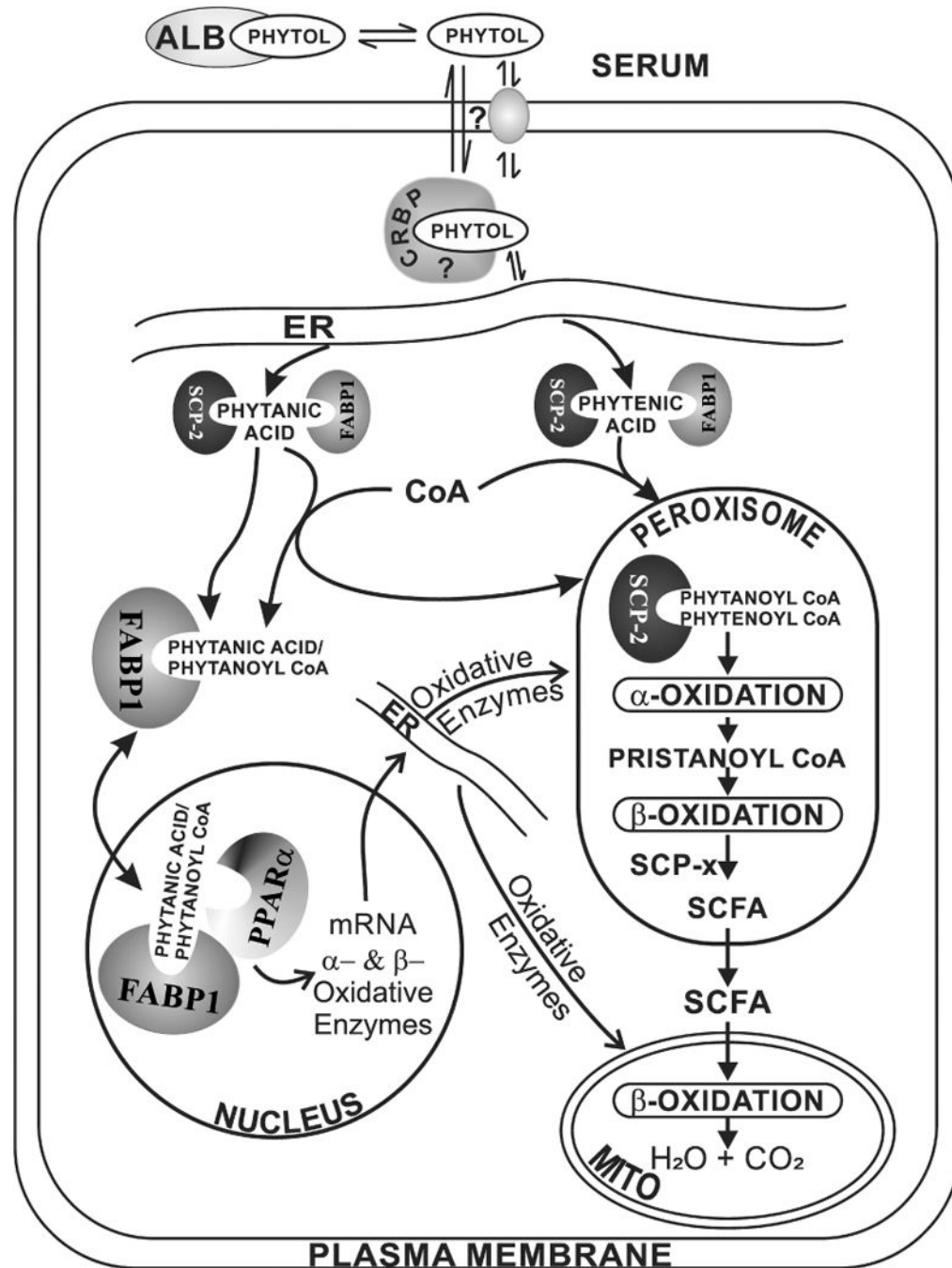


Fig. 7. Proposed pathway whereby *Fabp1* and *Scp-2/Scp-x* gene products facilitate hepatic phytol metabolism

In serum, phytol is bound to albumin [64]. Phytol dissociates from albumin-phytol complexes for uptake across the hepatocyte plasma membrane (PM) by as yet unknown mechanism(s) (e.g. diffusional, carrier mediated). While it is not known how the poorly aqueous-soluble phytol traffics to the endoplasmic reticulum (ER), it is not mediated by FABP1 or SCP-2 since neither binds phytol. Nevertheless, due to its insolubility a carrier protein is likely required, potentially cellular retinol binding protein (CRBP) or another cytosolic carrier protein. At the ER, phytol is metabolized to phytanic acid and phytenic acid

—both of which are bound by FABP1 (the most prevalent lipidic carrier/chaperone protein in liver, highly localized in cytosol [65, 66]) as well as SCP-2 (several fold less present than FABP1 in liver, equally distributed between cytosol and peroxisomes [9–11]). FABP1 and SCP-2 then transport bound phytanic acid and phytanic acid to the peroxisomal membrane for conversion to/internalization of their respective CoA thioesters. Peroxisomally localized SCP-2 [9–11] then binds phytanoyl-CoA and phytanoyl-CoA [5, 6]. It is important to note that, with some exception [67], there is little evidence for FABP1 localization within peroxisomes [65, 66]. Within the peroxisomal matrix SCP-2 then facilitates peroxisomal oxidation of phytanoyl-CoA and phytanoyl-CoA by directly interacting with and transporting the bound ligands to oxidative enzymes. For example, *in vitro* studies show that SCP-2 stimulates peroxisomal phytanoyl-CoA 2-hydroxylase which is the key enzyme and first step in peroxisomal α -oxidation of branched-chain fatty acids [7, 12]. Downstream of this step, the other *Scp-2/Scp-x* gene product (i.e. SCP-x, exclusively peroxisomal) is the only known branched-chain 3-ketoacyl CoA thiolase [4, 9, 60, 68]. Several cycles of α - and β -oxidation then successively shorten the branched-chain fatty acids to short chain fatty acids (SCFA) less than 12 carbons long. SCFAs are not bound by either SCP-2 [5, 23] or FABP1 [69–72], but instead readily diffuse across the peroxisomal membrane into the cytosol and subsequently across the mitochondrial membranes for completion of β -oxidation within the mitochondrial matrix.